Article

Preparation of High Quality Electrical Insulator Self-Assembled Monolayers on Gold. Experimental Investigation of the Conduction Mechanism through Organic Thin Films

Steffen Maisch, Frank Buckel, and Franz Effenberger

J. Am. Chem. Soc., **2005**, 127 (49), 17315-17322• DOI: 10.1021/ja0548992 • Publication Date (Web): 18 November 2005

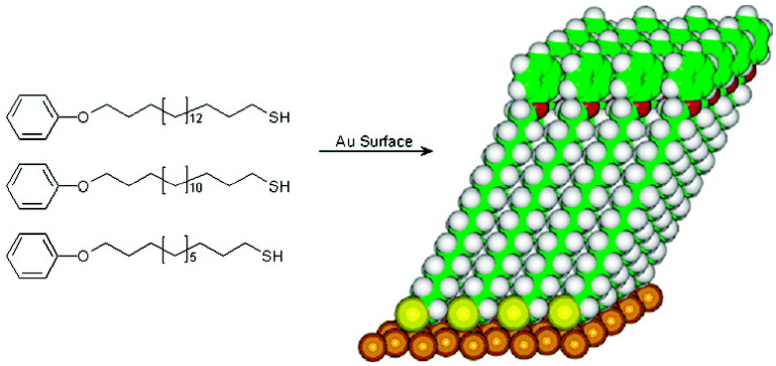

More About This Article

Additional resources and features associated with this article are available within the HTML version:

- Supporting Information
- Links to the 5 articles that cite this article, as of the time of this article download
- Access to high resolution figures
- Links to articles and content related to this article
- Copyright permission to reproduce figures and/or text from this article

View the Full Text HTML

J|A|C|S
ARTICLES
Published on Web 11/18/2005

Preparation of High Quality Electrical Insulator Self-Assembled Monolayers on Gold. Experimental Investigation of the Conduction Mechanism through Organic Thin Films

Steffen Maisch, Frank Buckel, and Franz Effenberger*

Contribution from the Institut für Organische Chemie, Universität Stuttgart, Pfaffenwaldring 55, D-70569 Stuttgart, Germany

Received July 21, 2005; E-mail: franz.effenberger@oc.uni-stuttgart.de

Abstract: Self-assembled monolayers (SAMs) form highly ordered, stable dielectrics on conductive surfaces. Being able to attach larger-area contacts in a MIM (metal−insulator-metal) diode, their electrical properties can be determined. In this paper, the electrical conduction through thiolate SAMs of different alkyl chain lengths formed on gold surfaces were studied and discussed. The influence of the headgroup with respect to the surface quality and prevention of short circuits is investigated. Phenoxy terminated alkanethiols were found to form high quality SAMs with perfect insulating properties. Synthesis of the required terminally substituted long chain thiols have been developed. The *I*(*V*) characteristics of MIM structures formed with these SAMs are measured and simulated according to theoretical tunneling models for electrical conductivity through thin organic layers. SAM based electronic devices will become especially important for future nanoscale applications, where they can serve as insulators, gate dielectric of FETs, resistors, and capacitor structures.

Introduction

The development of ultrathin insulators with high stability against electrical breakdown is a decisive problem in nanoelectronics.[2] Today, the two electrode surfaces in commercially available thin film capacitors are normally separated by polymers of micrometer thickness. Mann and Kuhn[3] were the first who investigated electrical conduction through Langmuir−Blodgett (LB) monolayers sandwiched between two metal electrodes. They observed an exponential dependence of the dc conductivity (σ) on the fatty acid chain length at room temperature and at −35 °C. From these results, they proposed a tunneling mechanism through fatty acid monolayers. To gain better insight into the mechanism of electrical conduction, Sagiv et al. studied ⟨Al-adsorbed monolayer-Al⟩ junctions.[4] Adsorbed monolayers of saturated fatty acids (14 to 23 C-atoms), short chain perfluorinated acids (7 to 10 C-atoms) and *n*-octadecyltrichlorosilane gave the following results: At room temperature there was no definite relation between the dc conductivity and the length of the fatty acid. At 77 K and lower temperature, however, an exponential dependence on the chain length could be observed. These results suggest that only at lower temperature the conduction through the monolayer agrees with the tunneling mechanism. The barrier height was estimated to be approximately 2.8 and 5.2 eV for fatty acids and perfluorinated fatty acids, respectively.[4]

Within the past few years great advances in the preparation of self-assembled monolayers as well as in the determination of their structure and their chemical and physical properties have been achieved.[5] From a great number of investigations, it is known that long-chain alkyl monolayers have excellent insulating properties. However, due to the difficulties involved in producing monolayers of good quality and reproducibility meaningful results concerning electrical conductivity have not always been achieved.

Since in this paper exclusively investigations on the electrical conductivity of ⟨gold-SAM-metal (electrolyte)⟩ junctions are reported, only the literature of these and closely related systems will be discussed.

A relatively simple method for the generation of a junction ⟨gold-SAM-metal⟩ is to use an STM tip as the counter electrode of an alkanethiol SAM on gold.[6,7] This conductivity system was applied to mixed layers from alkanethiols and long-chain conjugated π-systems (e.g., oligophenylethinyl derivatives). From STM imaging an electron transfer from the gold surface to the STM tip via the conjugated π-systems was proposed.[6a,b,h,7e]

Besides the direct application of the STM tip as counter electrode also ⟨gold-SAM-metal cluster-STM tip⟩ junctions were intensively investigated with respect to the electrical properties

(1) (a) Maisch, S. Diplomarbeit, Universität Stuttgart 2000, and Dissertation in preparation. (b) Buckel, F. Dissertation, Universität Stuttgart 2000.
(2) (a) Kuhn, H. *Pure Appl. Chem.* **1981**, *53*, 2105−2122. (b) Tieke, B. *Adv. Mater*. **1990**, *2*, 222−231. (c) Ratner, M. A.; Jortner, J. *Molecular Electronics*; Blackwell Science Ltd.: London, 1997.
(3) Mann, B.; Kuhn, H. *J. Appl. Phys.* **1971**, *42*, 4398−4405.
(4) Polymeropoulos, E. E.; Sagiv, J. *J. Chem. Phys.* **1978**, *69*, 1836−1847.
(5) (a) Bain, C. D.; Whitesides, G. M. *Angew. Chem., Int. Ed. Engl.* **1989**, *28*, 506−512. (b) Ulman, A. *Chem. Rev.* **1996**, *96*, 1533−1554. (c) Schreiber, F. *Progress Surf. Sci.* **2000**, *65*, 151−256. (d) McCreery, R. L. *Chem. Mater.* **2004**, *16*, 4477−4496.

10.1021/ja0548992 CCC: $30.25

of SAMs.[7] So, for example, nanometer-sized gold clusters have been deposited from a cluster beam onto thiol terminated SAMs.[7a,b] The deposition of metal clusters on SAMs can, however, also be performed by chemical reduction of metal salts[7c] or by electrodeposition.[8] The replacement of the STM tip as counter electrode could be realized directly with ⟨gold-SAM-metal⟩ junctions,[9] prepared, for example, by evaporation of titanium onto a 4-phenylthiophenolate-SAM,[9b] whereby the area of contact is restricted to ≤30 nm diameter. The electrical properties of these systems have not been reported. A further ⟨metal−insulator-metal⟩ junction has been assembled by deposition of silver paint on top of a gold-octadecanethiol SAM surface, showing that the SAM increased the resistance of the device by 10 orders of magnitude compared to devices without monolayer.[10]

The most important method for measuring rates of electron transport across organic thin films has been established by Whitesides et al. using ⟨Hg−SAM||SAM-metal⟩ junctions.[11a−c]

The current that flows across these junctions depends both on the molecular structure and on the thickness of the SAMs. The current density decreased with increasing distance between the electrodes. From the experimental results, it was concluded that the mechanism of electron transport is super exchange tunneling. The absolute magnitude of the current density in these junctions is in agreement with the results of ⟨Hg−SAM||SAM-Hg⟩ junctions described by Majda et al.[12] These junctions using a SAM supported on the surface of a drop of mercury provide an interesting test bed for screening the intrinsic electrical properties of SAMs, but they probably cannot be developed into practically useful microelectronic components. Besides the difficulty in handling electronic devices containing liquid Hg electrodes, these junctions show a relatively low electrical breakdown voltage (BDV),[11] a severe disadvantage for the application of SAMs as insulators. The BDV is revealed by an abrupt increase in current flowing across the junction in response to increasing the applied potential. The BDV depends expectedly on the thickness and the tilt angle of SAMs but also on the type of the metals applied as electrodes (Au, Au/Hg, Cu, Hg, Ag).[11a] Interestingly, a dependence of BDV on the chemical structure of SAMs was not observed so far, SAMs composing aliphatic or aromatic residues, respectively, do not differ in BDV.[11]

Chart 1

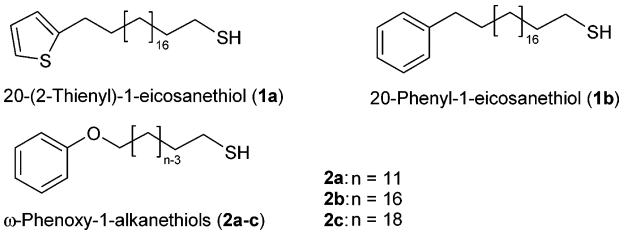

The practically most simple method to prepare ⟨gold-SAM-metal⟩ junctions appears to be undoubtedly the evaporative deposition of metals onto gold-SAM surfaces. Penetration of metal atoms and metal clusters, respectively, into the monolayer, resulting in electrical short circuits, has probably prevented a general application of this method.[13] Penetration of metals into SAMs might be hindered by SAMs with functionalized surfaces (e.g., with COOH end groups), which are capable of reacting with metals,[13] or by decreasing the temperature during the evaporation process.[14] Interestingly, SAM forming molecules with methyl side groups have fewer defects than SAMs of comparable *n*-alkanethiols.[13c]

In the present publication, we report on the preparation and the properties of ⟨gold-SAM-metal⟩ junctions with highly ordered SAMs of ω-substituted alkanethiols such as **1** and **2** (Chart 1) where the ω-substituents are aromatic or heteroaromatic residues capable of giving strong π-electron interactions (π-stacking).[15] These junctions surprisingly show no electrical short circuits in large-area and have a markedly increased electrical breakdown voltage. They should therefore have decisive advantages for various applications in electronic devices. These stable systems should also enable to determine the mechanism of electron transport through organic thin films experimentally without any of the assumptions necessary for other systems applied until now.[11,12]

Results and Discussion

Synthesis of the Thiols 2a−c. While the synthesis of the thiols **1a,b** has been published already,[16a] the phenoxy-terminated thiols **2a−c** were prepared as outlined in Scheme 1.

The known bromoalkenes **3a** and **3b,c**[16b] have been reacted with potassium phenolate, prepared from potassium methanolate

(6) (a) Bumm, L. A.; Arnold, J. J.; Cygan, M. T.; Dunbar, T. D.; Burgin, T. P.; Jones II, L.; Allara, D. L.; Tour, J. M.; Weiss, P. S. *Science* **1996**, *271*, 1705−1707. (b) Cygan, M. T.; Dunbar, T. D.; Arnold, J. J.; Bumm, L. A.; Shedlock, N. F.; Burgin, T. P.; Jones II, L.; Allara, D. L.; Tour, J. M.; Weiss, P. S. *J. Am. Chem. Soc.* **1998**, *120*, 2721−2732. (c) Datta, S.; Tian, W.; Hong, S.; Reifenberger, R.; Henderson, J. I.; Kubiak, C. P. *Phys. Rev. Lett.* **1997**, *79*, 2530−2533. (d) Dhirani, A.; Lin, P.-H.; Guyot-Sionnest, P.; Zehner, R. W.; Sita, L. R. *J. Chem. Phys.* **1997**, *106*, 5249−5253. (e) Bumm, L. A.; Arnold, J. J.; Dunbar, T. D.; Allara, D. L.; Weiss, P. S. *J. Phys. Chem. B* **1999**, *103*, 8122−8127. (f) Fan, Fu-R. F.; Yang, J.; Cai, L.; Price, D. W., Jr.; Dirk, S. M.; Kosyukin, D. V.; Yao, Y.; Rawlett, A. M.; Tour, J. M.; Bard, A. J. *J. Am. Chem. Soc.* **2002**, *124*, 5550−5560. (g) James, D. K.; Tour, J. M. *Chem. Mater.* **2004**, *16*, 4423−4435. (h) Wakamatsu, S.; Akiba, U.; Fujihira, M. *Jpn. J. Appl. Phys.* **2002**, *41*, 4998−5002.
(7) (a) Dorogi, M.; Gomez, J.; Osifchin, R.; Andres, R. P.; Reifenberger, R. *Phys. Rev.* **1995**, *B52*, 9071−9077. (b) Andres, R. P.; Bein, T.; Dorogi, M.; Feng, S.; Henderson, J. I.; Kubiak, C. P.; Mahoney, W.; Osifchin, R. G.; Reifenberger, R. *Science* **1996**, *272*, 1323−1325. (c) Grummt, U.-W.; Geissler, M.; Drechsler, T.; Fuchs, H.; Staub, R. *Angew. Chem., Int. Ed. Engl.* **1998**, *37*, 3286−3289. (d) Beebe, J. M.; Eugelkes, V. B.; Miller, L. L.; Frisbie, C. D. *J. Am. Chem. Soc.* **2002**, *124*, 11268−11269. (e) Engelkes, B. V.; Beebe, J. M.; Frisbie, C. D. *J. Am. Chem. Soc.* **2004**, *126*, 14287−14296.
(8) Cavalleri, O.; Bittner, A. M.; Kind, H.; Kern, K.; Greber, T. *Z. Phys. Chem.* **1999**, *208*, 107−136.
(9) (a) Reed, M. A.; Zhou, C.; Muller, C. J.; Burgin, T. P.; Tour, J. M. *Science* **1997**, *278*, 252−254. (b) Zhou, C.; Deshpande, M. R.; Reed, M. A.; Jones, L., II; Tour, J. M. *Appl. Phys. Lett.* **1997**, *71*, 611−613.
(10) Baker, M. V.; Landau, J. *Aust. J. Chem.* **1995**, *48*, 1201−1211.
(11) (a) Haag, R.; Rampi, M. A.; Holmlin, R. E.; Whitesides, G. M. *J. Am. Chem. Soc.* **1999**, *121*, 7895−7906. (b) Holmlin, R. E.; Haag, R.; Chabinyc, M. L.; Ismagilov, R. F.; Cohen, A. E.; Terfort, A.; Rampi, M. A.; Whitesides, G. M. *J. Am. Chem. Soc.* **2001**, *123*, 5075−5085. (c) Holmlin, R. E.; Ismagilov, R. F.; Haag, R.; Mujica, V.; Ratner, M. A.; Rampi, M. A.; Whitesides, G. M. *Angew. Chem., Int. Ed.* **2001**, *40*, 2316−2320.
(12) (a) Slowinski, K.; Chamberlain II, R. V.; Bilewicz, R.; Majda, M. *J. Am. Chem. Soc.* **1996**, *118*, 4709−4710. (b) Slowinski, K.; Fong, H. K. Y.; Majda, M. *J. Am. Chem. Soc.* **1999**, *121*, 7257−7261. (c) Slowinski, K.; Chamberlain, R. V.; Miller, C. J.; Majda, M. *J. Am. Chem. Soc.* **1997**, *119*, 11910−11919.
(13) (a) Jung, D. R.; Czanderna, A. W. *Crit. Rev. Solid State Mater. Sci.* **1994**, *19*, 1−54. (b) Herdt, G. C.; King, D. E.; Czanderna, A. W. *Z. Phys. Chem.* **1997**, *202*, 163−196. (c) Braach-Maksvytis, V.; Raguse, B. *J. Am. Chem. Soc.* **2000**, *122*, 9544−9545.
(14) Tarlov, M. J. *Langmuir* **1992**, *8*, 80−89.
(15) (a) Hunter, C. A.; Lawson, K. R.; Perkins, J.; Urch, C. J. *J. Am. Chem. Soc. Perkin Trans* **2001**, 651−669 (b) Whitten, D. G.; Chen, L.; Geiger, H. C.; Perlstein, J.; Song, X. *J. Phys. Chem. B* **1998**, 10098−10110.
(16) (a) Buckel, F.; Persson, P.; Effenberger, F. *Synthesis* **1999**, 953−958. (b) Effenberger, F.; Heid, S. *Synthesis* **1995**, 1126−1130. (c) Seifritz, S. Dissertation, Universität Stuttgart 2001. (d) Aggarwal, V. K.; Angelaud, R.; Bihan, D.; Blackburn, P.; Fieldhouse, R.; Fonquerna, S. J.; Ford, G. D.; Hynd, G.; Jones, E.; Jones, R. V. H.; Jubault, P.; Palmer, M. J.; Ratcliffe, P. D.; Adams, H. *J. Chem. Soc., Perkin Trans. 1* **2001**, 2604−2622.

Scheme 1. Reflexion Spectrum of the SAM Formed from Compound 2c on Gold.

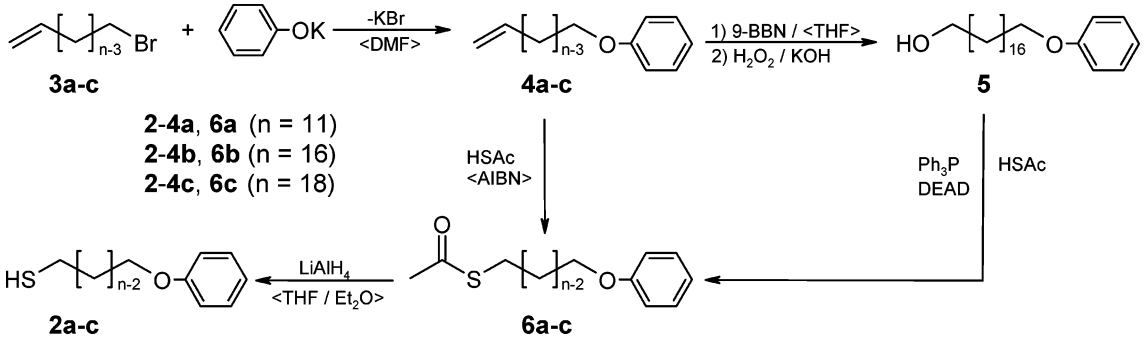

and phenol, in DMF[16c] to give the alkenylphenyl ethers **4a**−**c**, which were isolated after chromatographic purification in 79−92% yield. The terminal thioacetate function was introduced by addition of thioacetic acid to the alkenes **4a**−**c** using azoisobutyronitrile (AIBN) as radical initiator at 60 °C.[16d] The thioacetates **6a**−**c** were obtained in 69−85% yield after chromatography on silica gel. An alternative route to the thioacetates **6a**−**c** is shown in Scheme 1 for the preparation of **6c**. In a modified known procedure,[16a] phenoxy-substituted octadecene **4c** was hydroborated with 9-borabicyclo[3.3.1]nonane (9-BBN)[17] and subsequently oxidized with H_2O_2 to give the corresponding alcohol **5** in 64% yield. Analogously to a literature procedure,[16a] the alcohol **5** was converted in a Mitsunobu reaction with triphenylphosphine/diethyl azodicarboxylate (DEAD) and thioacetic acid to give **6c** in an overall yield of 39%. The thiols **2a**−**c** were eventually obtained by reduction of the thioacetates **6a**−**c** with $LiAlH_4$.[16a]

Preparation and Characterization of the Thiol Monolayers (SAMs) on Gold Surfaces. Commercial gold substrates were either pretreated according to a known procedure[18] or cleaned with "piranha acid" (33% H_2O_2/concentrated H_2SO_4 3:7) and subsequently tempered on a heating plate for 24 h at 380 °C. To smooth the surface roughness, the gold wafers were connected as anode in an electrolyte containing tetrachloroauric-(III) acid versus platinum as cathode, whereby the gold surface was partly electrolytically dissolved within 72 h using a sine alternating voltage (2.4 Vpp). For the monolayer preparation the gold substrates were immersed in a solution of the thiols **1** and **2**, respectively, in ethanol for 24 h. After cleaning and drying, the samples were characterized by X-ray photoelectron (XPS) and FTIR spectroscopy as well as by water advancing contact angle measurement.

Monolayer assemblies of **1a,b** with a film thickness of about 30 Å are bound to the gold surface via thiolate as confirmed by XPS.[19] For the monolayers of both **1a,b**[19c] and **2a**−**c** contact angles in the range of 90−96° were determined. From the position of the asymmetric stretching vibration band ($\nu_{as}(CH_2)$) at 2917−2918 cm^{-1}, densely packed, well ordered monolayers of thiols **1a**−**c** and **2a,b** with estimated tilt angles of 37−40° were deduced.[19c] A nearly perpendicular orientation of the phenyl ring to the gold surface, diminishing the space requirement and improving phenyl−phenyl interactions, was concluded from the $\nu(C{=}C)_{aryl}$ vibration band at 1498 cm^{-1} with an intensity comparable to the intensity of the symmetric $\nu_s(CH_2)$ band in the reflection absorption IR (RAIR) spectra of SAMs of **1b**.[19c] In KBr pellets the intensity of the $\nu(C{=}C)_{aryl}$ band is considerably weaker than the intensity of the $\nu_s(CH_2)$ band.[19c]

Preparation and *I*(*V*) Characteristics of ⟨Gold-SAM-Al⟩ Junctions (Method A). The ⟨gold-SAM-Al⟩ junctions were prepared as follows: aluminum contacts with 0.5 mm diameter and 250−260 nm height were built by thermal evaporation of aluminum under vacuum (10^{-6} mbar) through a mask on top of the SAMs of the aryl terminated compounds **1a,b** on gold, at a deposition rate of approximately 5 nm s^{-1}. A reproducible insulator behavior of the roughly 3 nm thick SAMs in the ⟨gold-SAM **(1)**−Al⟩ junctions was unambiguously ascertained for numerous contacts (about 30−50% of the measured Al dots), whereby a current only in the range of nA was measured at a dc voltage of ±1 V. On the contrary, in comparable junctions with methyl terminated SAMs (obtained with eicosanethiol on gold), already at very low voltage ($<\pm$0.1 V) a current in the range of amperes was measured for all aluminum dots, indicating many short circuits, and thus these methyl terminated SAMs show no insulator behavior.

Although the ⟨gold-SAM-Al⟩ junctions described so far show the decisive influence of terminal substituent of SAMs on the *I*(*V*) characteristics, this method to build up junctions has disadvantages. The evaporative aluminum deposition obviously still allows metal penetration into the monolayer.[20] Even in aryl terminated SAMs, electrical short circuits in roughly 50% of the samples have been measured as mentioned above. We therefore were interested in developing other methods to prepare ⟨gold-SAM-metal⟩ junctions with perfect insulating behavior in all cases.

Preparation and Conductivity Measurements of ⟨Gold-SAM-Metal (Electrolyte)⟩ Junctions (Method B). To exclude metal penetration during the evaporation process the metal deposition onto self-assembled monolayers by means of electrolysis and contacting with electrolyte solution appeared to be promising, because of the even current distribution over relatively large areas provided by the bulk electrolyte. Therefore, we studied the cathodic deposition of thin films of noble metals (e.g., Au) from the respective electrolyte solution on the monolayer surface at a very low current which had to pass through the SAM. Thereby electrochemical redox reactions which might contribute to damage the SAM had to be avoided. The SAM coated gold wafers were electrolyzed in the electrolyte

(17) Thomas, N. E. In *Organic Synthesis: The Roles of Boron and Silicon*; Davies, S. G., Ed.; Oxford University Press: Oxford, 1991, p 10.
(18) Ron, H.; Mattis, S.; Rubinstein, J. *Langmuir* **1998**, *14*, 1116−1121.
(19) (a) Sellers, H.; Ulman, A.; Shnidman, Y.; Eilers, J. E. *J. Am. Chem. Soc.* **1993**, *115*, 9389−9401. (b) Castner, D. G.; Hinds, K.; Grainger, D. W. *Langmuir* **1996**, *12*, 5083−5086. (c) Buckel, F.; Effenberger, F.; Yan, C.; Gölzhäuser, A.; Grunze, M. *Adv. Mater.* **2000**, *12*, 901−905.
(20) Fisher, G. L.; Walker, A. V.; Hooper, A. E.; Tighe, T. B.; Bahnek, K. B.; Skriba, H. T.; Reinard, M. D.; Haynie, B. C.; Opila, R. L.; Winograd, N.; Allara, D. L. *J. Am. Chem. Soc.* **2002**, *124*, 5528−5541.

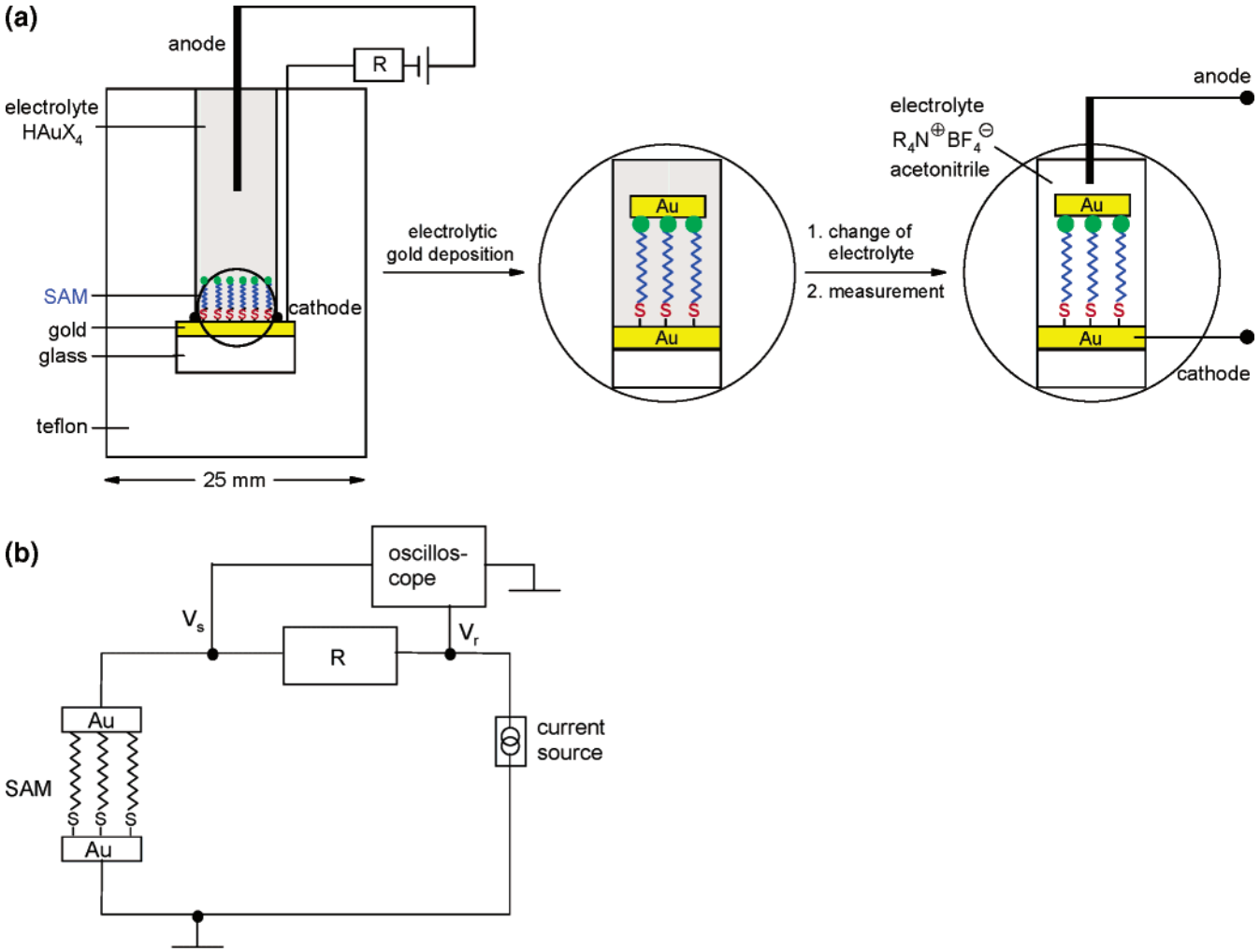

Figure 1. **(a)** Schematic illustration of the electrochemical preparation and the conductivity measurements of ⟨gold-SAM-gold⟩ junctions. **(b)** Schematic illustration of the measuring principle. Voltage at the sample (V_S), voltage proportional to current (V_R), current source (Norton source) generating short pulses of increasing current.

solution containing tetrachloroauric(III) acid in acetonitrile at direct current (≤0.5 V) for 5 days (Figure 1a). This slow deposition avoids damage to the SAM, whereas a fast deposition led to the buildup of Au crystallites resulting in short circuits. The electrolytic cell, which consists of a carefully designed Teflon tube and screw, with the ⟨gold-SAM-metal⟩ junctions prepared as described, was then carefully rinsed with water and filled with supporting electrolyte for the measurement of $I(V)$ characteristics (Figure 2). The gold wafer is contacted by a platinum wire inside the Teflon screw bottom which touches its surface only outside the active area to prevent any mechanical stress or scratches on the measured SAM surface, while the anode is a gold-plated platinum wire. The $I(V)$ curves for higher voltages from 0 to 10 V were obtained by applying a Norton source of high output impedance which programs a constant current (Figure 1b). The BDV in all cases measured was higher than 15 V which corresponds to an amazingly high electrical field strength in the order of 50 MV/cm. Short pulses of increasing current were generated, and both the voltage at the sample and that proportional to the current flowing through the system were observed on a digital oscilloscope. At lower voltages (0 to 1.8 V), where dielectric breakdown is not a major problem, while low-noise experimental data are required for the exact evaluation of the conduction mechanism, several (64−256) measurements of the same sample were averaged to increase the signal-to-noise (Figure 3). These measurements were carried out by directly contacting the SAM by an electrolyte without intermediate gold layer.

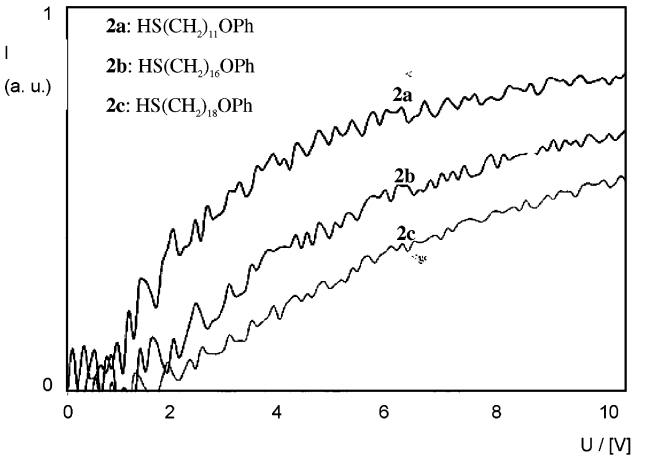

Figure 2. $I(V)$ characteristics of the ⟨gold-SAM **2a**−**c**-gold (electrolyte)⟩ junctions in the range of 0 to 10 V.

Discussion of the Influence of the Chemical Structure on the Insulating Properties and the Electrical Breakdown of

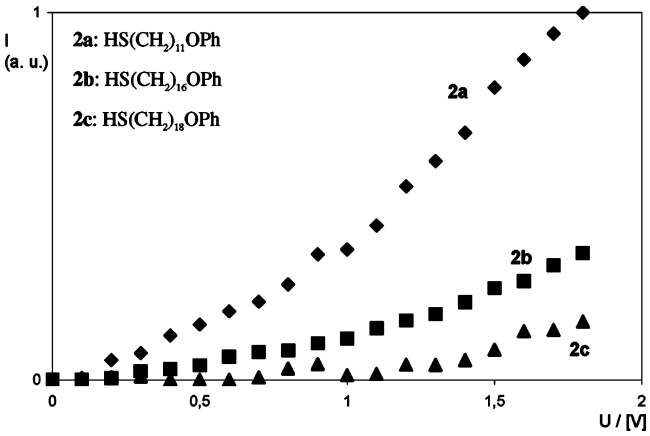

Figure 3. Averaged $I(V)$ characteristics of the ⟨gold-SAM **2a**−**c**-electrolyte⟩ junctions in the range 0 to 1.8 V.

⟨Gold-SAM-Metal⟩ Junctions. By applying ω-aryl substituted SAMs (compounds **1a**,**b** and **2**) and electrolytic deposition of the counter electrode according to method B we succeeded in the preparation of ⟨gold-SAM-metal⟩ junctions without any pinholes, domain formation or impurities in large-area ($\geq$30 mm^2), and thus resulting in completely reproducible conductivity measurements through SAMs. Since these ⟨gold-SAM-metal⟩ junctions are stable at room temperature for several weeks and easy to handle, they are best suitable for fundamental investigations on the mechanism of electrical conduction through thin organic layers discussed in the next chapter. In this chapter especially the influence of the chemical structure and the sterical arrangement of the monolayers on the electrical insulator behavior is discussed.

In particular Whitesides et al.[11] reported comprehensively on the influence of the chemical structure of SAMs and the influence of various electrode metals on the BDV. From these investigations, it was inferred that the thickness of the ordered hydrocarbon layer is the major factor determining the BDV, and an exponentially dependence of the current density from the applied voltage was found. A linear dependence between thickness and BDV has been found for alkyl monolayers on a hydrogen terminated Si(111).[21] The tilt angle of SAMs versus the surface normal has also a strong influence. The BDV of alkanethiol SAMs on gold, with a tilt angle of ~30°, is lower by a factor of 2 than that on silver with a tilt angle of ~0°.[11c] The authors note that the value of BDV is surprisingly indifferent to the detailed structure of the molecules making up SAMs. There is no evidence that SAMs incorporating simple aromatic groups differ fundamentally in their electrical behavior from aliphatic SAMs.[11a] Because Whitesides et al. have investigated exclusively ⟨Hg−SAM || SAM-metal⟩ double junctions,[11] the obtained results cannot be transferred directly to our results of ⟨gold-SAM-metal⟩ junctions.

Recent investigations[19c] of the influence of aromatic groups incorporated in long-chain alkanethiol self-assembled monolayers on gold have shown that SAMs of both ω-phenyl eicosanethiol (**1a**) and 4-eicosylthiophenol consist of densely packed alkyl chains, independent of the position of the phenyl ring. Also the tilt angles in both cases are comparable. The decisive difference, however, is the orientation of the phenyl rings, elucidated mainly from RAIR spectra. In SAMs of **1a**, the phenyl moiety is nearly perpendicular to the surface normal,[19c] whereas in SAMs of 4-eicosylthiophenol, it is tilted.[19c]

(21) Zhao, J.; Uosaki, K.; *Appl. Phys. Lett.* **2003**, *83*, 2034−2036.

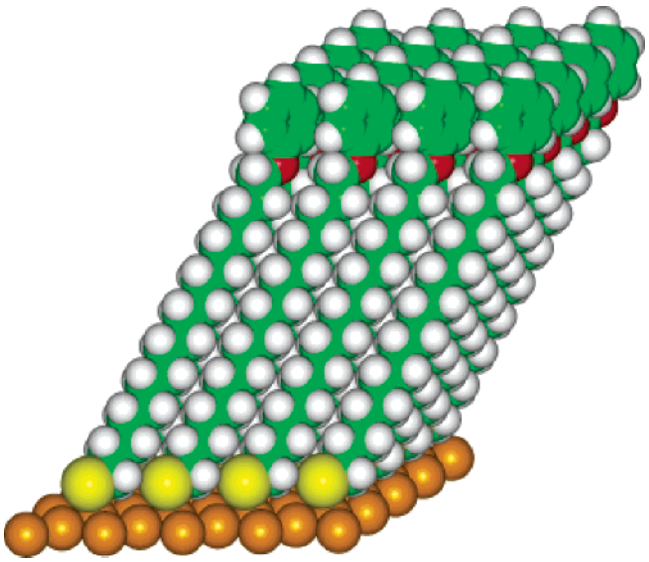

Figure 4. Molecular modeling of the SAM formed from **2c** on gold.

As can be shown by molecular modeling of the lateral SAM structure of compound **2c** on gold, a highly ordered system with optimal π-stacking (Figure 4) due to the more flexible ether bridge between the alkyl chain and the aromatic moiety is seen. This modeling was performed by the Cerius^2 software v. 4.2 from MSI using a cff 91 consistent force field and a rigid (1,0,0) gold surface. The phenoxy-phenoxy distances in both dimensions fit perfectly into the package of the alkyl chains and their placement on the gold surface.

From the presented structural investigations of SAMs of compounds **1a,b** and **2a**−**c** on gold we conclude that strong π-interactions of the terminal aromatic rings do not only favor the perfect order of SAMs but also "densify" their surface, markedly hindering the penetration of metals. The unusually high BDV values found for SAMs of compounds **1a,b** and **2a**−**c**, are assumed to arise also from the strong "densification" by π-stacking, although there is so far no unambiguous explanation or mechanism for the BDV of organic monolayers.[15a]

Experimental Evidence for the Tunneling Mechanism of the Electrical Conduction through Organic Monolayers. Among the different possible electrical conduction mechanisms discussed, the tunneling mechanism is most probable for thin organic films such as self-assembled monolayers. In nearly all publications dealing with this problem a tunneling mechanism is postulated for the electrical conductivity based on experimental data.[3,4,11,12] However, an unambiguous experimental evidence for the tunneling mechanism through organic monolayers was not yet possible, because up to now large-area measurements of $I(V)$ characteristics of ⟨metal-SAM-metal⟩ junctions could not be performed. The application of an electrolyte solution for contacting the SAM surface decreases the risk to measure current flowing through a short path in imperfections, because small pinhole-like defects have little influence. This is a result of the very slow diffusion process in geometrically small structures, whereas these defects give rise to low-impedance short circuits when metal as electrode is evaporated on the SAM.[9]

With the assumption of a tunneling mechanism for the electron transport through an insulator, e.g., thin organic layers, the tunneling probability and thus the electric current increase almost exponentially with decreasing thickness of the insulator,[20] while showing high dielectric strength.[21] Tunneling can occur through any kind of thin layer and was demonstrated in a heavily doped germanium diode by *Esaki*.[22c] In case of tunneling, electrons which do not have a potential large enough to overcome the barrier in a classical model can do so via tunneling. The tunneling probability for an electron and thus the current through the SAM depends on the applied voltage, the thickness of the barrier and its heigth.

The first can be varied with biasing while the properties of the SAM forming molecules determine the properties of the barrier. The insulator thickness is determined by the length of the SAM forming molecules. Under the assumption of a perfect square well potential with flat top and infinitely steep walls, the following formula is valid for the tunneling probability T[22d]

$$T = \frac{1}{1 + \frac{V^2}{4(VE - E^2)} \sinh^2 \sqrt{\frac{2md^2(V-E)}{\hbar^2}}} \qquad (1)$$

wherein V is the height of the barrier, m and E mass and energy of the electrons, respectively, and d the thickness of the layer. This formula is directly obtained by solving the Schroedinger equation for the assumed model without any approximations. In the given case, it can be approximated by an exponential function.[4] Here, (1) was used without further simplification. The insulator thickness d in self-assembled monolayers is defined by the chain length and the angle between chain and surface normal. In most investigations of the electron transport through organic monolayers this expected exponential dependence of current on the chain length was found.[3,4,11,12,22] The measurement of $I(V)$ characteristics of alkyl SAMs on silicon, performed by Vuillaume et al., however, deviate from this finding by showing a conductivity independent of the chain length, and the authors therefore exclude a tunneling mechanism.[23a]

In the preceding chapter, the conductivity through SAMs depending on the chain length of the SAM forming molecules and the bias was determined experimentally. On the basis of the thereby determined $I(V)$ characteristics a tunneling mechanism for the electron transport through SAMs will be proved in the following.

The experimentally obtained $I(V)$ characteristics of SAMs of compounds **2a**−**c** in ⟨gold-SAM-gold⟩ junctions are compared with the values expected theoretically for a tunneling mechanism. In the simplest case, a square-well potential is assumed for the course of the potential in the SAM in the zero-bias case (Figure 6a). The lengths l of the molecules result from molecular modeling.[22] The thickness of the potential barrier calculated by multiplying this value by the cosine of the tilt angle of 30° under the assumption that tunneling occurs through the bulk material and not along the single molecules. The barrier height is determined by comparing the experimentally found curves with the calculated ones: the sum of the residues at discrete measuring points in the range of 0−1.5 V is minimized. In the case of SAMs of thiols **2a**−**c**, experimental data and calculation, however, do not agree as can be demonstrated in Figure 5.

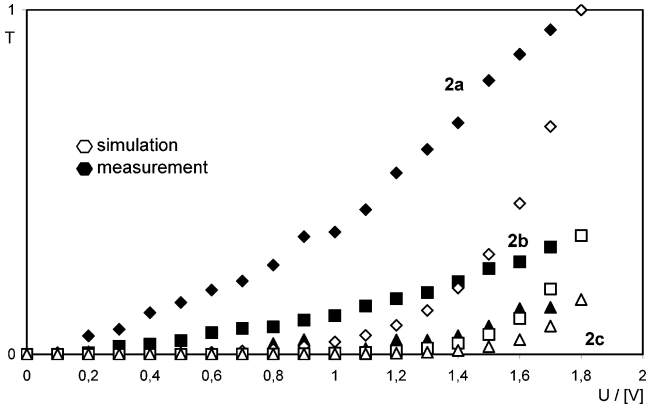

Figure 5. Measurement and comparisation with simulated tunneling through a square well barrier.

An optimal accordance of experimental results with calculations can be achieved however, if the potential of each methylene group in the alkyl chains is additionally modulated as shown in Figure 6a.[23]

The Schrödinger equation of this model is solved and optimized to the lowest sum of residues in comparison with experimental data. In case of a simple square potential, the calculated curve is obtaind from eq 1, while in case of the modulated potential (Figure 6), the resulting Schrödinger equations are solved numerically. Table 1 shows the results together with the modeled molecule lengths (PM3), measured from the thiol sulfur to the 4′-hydrogen atom of the phenyl rings, and the relative currents measured at $V = 0.8$ V. For the simulation, not the molecule lenghs l, but the thickness of the SAMs, $d = l \cos(30°)$, are used. From the obtained values, the theoretical tunneling curves can be simulated and compared with the experimental ones. In Figure 6b, the experimental curves are plotted together with the simulation. It shows considerable better agreement in the case of the modulated potential than the simple square well shape (Figure 6a).

Experimental Section

General Methods. Melting points were determined on a Büchi SMP 20 apparatus and are uncorrected. ^{1}H NMR spectra were recorded on a Bruker AC 250 F (250 MHz). Chemical shifts are given with TMS as an internal standard. Preparative column chromatography was performed on silica gel S, grain size 0.032−0.063 mm (Riedel-de Haen). Mass spectrometric data were obtained with a Finnigan MAT 711 or Finnigan MAT 95 mass spectrometer. Spectroscopic and analytical data are offered as Supporting Information. $I(V)$ characteristics were measured using a Tektronix Digital TDS 210 Oscilloscope.

Gold substrates were purchased from Metallhandel Schröer GmbH. On a 1 cm^2 glass slide a chromium layer was deposited and subsequently the gold layer prepared by high vacuum evaporation.

General Procedure for the Preparation of the Alkenylphenyl Ethers 4a−c. To a solution of phenol (1.30 g, 13.80 mmol) in dry dichloromethane (10 mL) under N_2 atmosphere was added potassium methanolate (0.90 g, 12.81 mmol). The reaction mixture was stirred at room temperature for 30 min and concentrated under vacuum. The remaining potassium phenolate was dissolved in dry DMF (6 mL), and

(22) (a) Mikkelsen, K. V.; Ratner, M. A. *Chem. Rev.* **1987**, *87*, 113−153 (b) York, R. L.; Nguyen, Ph. T.; Slowinski, K. *J. Am. Chem. Soc.* **2003**, *125*, 5948−5953. (c) Esaki, L. *Phys. Rev.* **1958**, *109*, 603. (d) Schwabl, F. *Quantum Mechanics*; Springer: New York **1992**, 59−65.

(23) (a) Boulas, C.; Davidovits, J. V.; Rondelez, F.; Vuillaume, D. *Phys. Rev. Lett.* **1996**, *76*, 4797−4800. (b) Vuillaume, D.; Boulas, C.; Collet, J.; Allan, G.; Delevue, C. *Phys. Rev B* **1998**, *58*, 16491−16498. (c) Gu, Y.; Akhremitcher, B.; Walker, G. C.; Waldeck, D. H. *J. Phys. Chem. B* **1999**, *103*, 5220−5226. (d) Selzer, Y.; Salomon, A.; Cahen, D. *J. Am. Chem. Soc.* **2002**, *124*, 2886−2887.

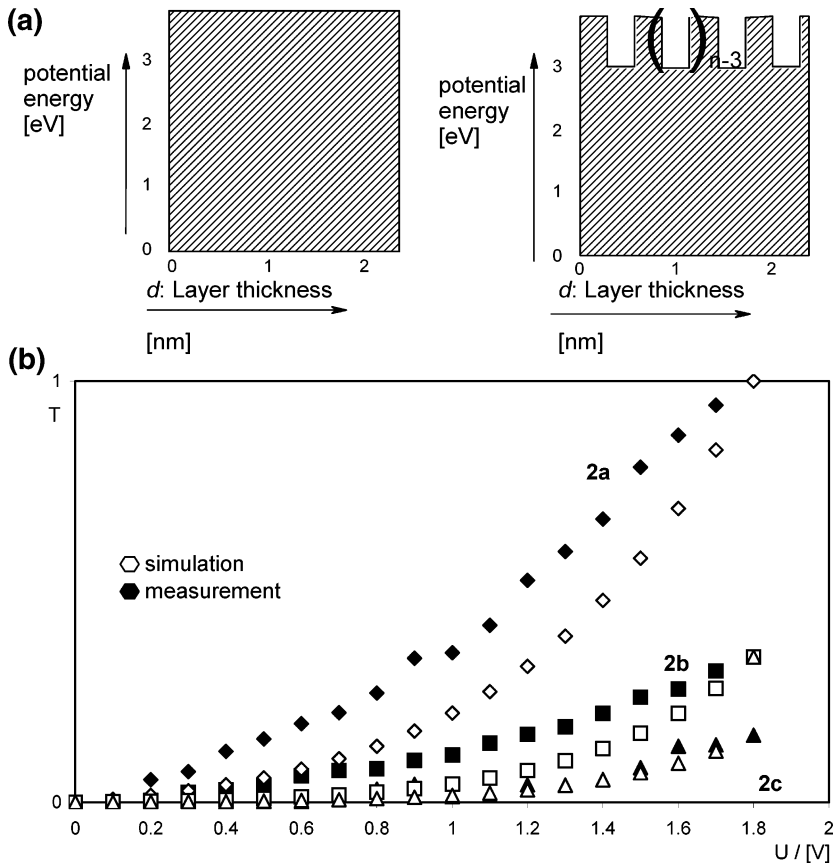

Figure 6. **(a)** Square well potential and potential modulated by addition of the dielectrics of the single methylene groups of the alkyl chains. **(b)** Measurement and comparisation with simulated tunneling through the barrier of part **a**.

Table 1. Comparisation of the Results of Tunneling Evaluation with the Potential Models According to Figure 6a

SAM forming compound	molecule length / by molecular modeling (PM3) (nm)	relative current at $V = 0.8$V	error of simulation (sum of residues) case 5	error of simulation (sum of residues) case 6
2a	1.63	1.00	1.68	0.340
2b	2.42	0.31	0.22	0.060
2c	2.67	0.12	0.02	0.003

the respective bromide **3a**−**c** (9.86 mmol) was added by syringe. After being stirred at 65 °C for 3 h and at room temperature for a further 12 h, to the reaction mixture was added dichloromethane and water (60 mL each) to solve precipitated potassium bromide. The phases were separated and the organic layer was washed five times with water (60 mL), dried (Na_2SO_4), filtered through a silica gel column (×5 cm) and eluted with dichloromethane/petroleum ether (1:1) (TLC. control). Evaporation gave the products **4a**−**c**.

4a: yield 2.16 g (89%) as a colorless liquid; **4b**: yield 2.47 g (79%) as a white solid; mp 34 °C; **4c**: yield 3.13 g (92%) as a white solid; mp 44 °C.

General Procedure for the Preparation of the Phenoxyalkyl Thioacetates 6a−**c.** To a solution of the respective alkene **4a**−**c** (0.38 mmol) in chloroforme (4 mL) under N_2 atmosphere was added thioacetic acid (2.67 g, 35.1 mmol) and 4 mg α,α′-azo-isobutyronitrile (AIBN). After being heated at 60 °C for 24 h, the reaction mixture was concentrated under vacuum, and the light yellow residue was chromatographed on silica gel with dichloromethane/petroleum ether (1:1) to give the products **6a**−**c**.

6a: yield 85 mg (69%) as a yellow oil; **6b**: yield 127 mg (85%) as a white solid; **6c**: yield 120 mg (75%) as a white solid; mp 65 °C.

Alternative Preparation of 6c via 18-Phenoxyoctadecan-1-ol (5). (a) A solution of **4c** (3.45 g, 10.0 mmol) and 9-borabicyclononane (9-BBN) (20.0 mmol) in THF (40 mL) was refluxed under N_2 atmosphere for 7 d. Then a solution of KOH in H_2O_2 (33%), prepared from KOH (2.81 g, 50.0 mmol) and 10 mL H_2O_2 at 0 °C, was added at room temperature. The reaction mixture was stirred at 50 °C for 40 min. After being cooled (ice bath), 40 mL water were added followed by very slow addition of a solution of $CoCl_2 \cdot 6H_2O$ (0.3 g) in 2 mL water (O_2 generation). The reaction mixture was then acidified with H_2SO_4 (30%) and a solution of $FeSO_4 \cdot 7H_2O$ (0.5 g) in water (5 mL) was added. After being stirred for 12 h at room temperature, water was added, and the reaction mixture extracted with *tert*-butylmethyl ether in a perforator. The extract was dried (Na_2SO_4), concentrated under vacuum and chromatographed on silica gel with dichloromethane/petroleum ether (1:3) to give 2.32 g (64%) **5**.

(b) Thioacetate **6c** was prepared analogously to a known procedure[15a] from **5** (0.18 g, 0.50 mmol); yield: 0.128 g (61%).

General Procedure for the Preparation of Phenoxy-1-alkanethiols 2a−**c.** To a solution of the respective compounds **6a**−**c** (0.37 mmol) in diethyl ether/THF (1:1) (6 mL) was added solid $LiAlH_4$ (0.79 mmol, 30 mg) under N_2 atmosphere, and the reaction mixture stirred at room temperature for 1 h. The reaction mixture was first hydrolyzed with 1 mL of degassed water, and then with HCl (25%, 2 mL). Then 10 mL water and 15 mL dichloromethane were added. The phases were separated and the organic layer was washed with water (10 mL), and dried (Na_2SO_4). Concentration under vacuum gave products **2a**−**c**.

2a: yield 70 mg (61%) as a yellow oil; **2b:** yield 93 mg (72%) as light yellow solid; mp 55 °C; **2c**: yield 98 mg (70%) as light yellow solid; mp 60 °C.

Purification and Surface Treatment of Gold Substrates. Commercial gold substrates (12 × 12 × 1.1 mm borosilicate glass with chromium layer of 1−4 nm thickness as adhesion promoter and vaporcoated gold layer of 200−300 nm thickness) were cleaned with "piranha" acid (33% H_2O_2/concentrated H_2SO_4 3:7) for 15 min at 65

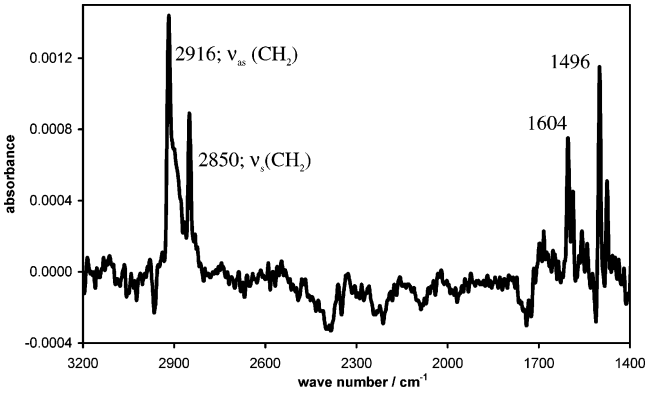

Figure 7. FT-IR reflexion spectrum of the SAM formed from compound **2c** on gold.

°C. The gold substrates were then tempered at 650 K for 24 h on a heating plate. To reduce the surface roughness, the substrates were treated in an electrolyte from tetrachloroauric(III) acid (0.08 g), NBu_4BF_4 (9.5 g), $Mg(NO_3)_2$ (1.2 g) in degassed acetonitrile (1 L) and connected as anode versus platinum at sine alternating voltage with interfered direct voltage for 72 h.

Monolayer Preparation. The cleaned gold substrates were immersed in a stirred solution of the respective thiol in absolute ethanol, degassed by three freeze−pump−thaw cycles (1 mM for **1a**,**b**, 0.5 mM for **2a**−**c**) under inert gas atmosphere for 24 h (**1a,b**) or 48 h (**2a**−**c**). Samples were rinsed with absolute dichloromethane and blown dry with nitrogen.

Spectroscopic Characterization. Figure 7 shows an FT-IR-spectrum of the SAM formed from compound **2c**.

Both the symmetric and asymmetric CH_2 valence vibrations at $\tilde{\nu}_s = 2850\ cm^{-1}$ and $\tilde{\nu}_{as} = 2916\ cm^{-1}$ are visible. They correspond to the values of the same compound in crystalline state, rather than in liquid. In the range from 1496−1604 cm^{-1} aromatic ring vibrations can be seen. The spectrum was taken by averaging 2000 scans of the same sample in an FT-IR spectrometer.

Cathodic Metal Deposition. The coated gold substrates in an electrolyte from tetrachloroauric(III) acid (0.9 g), $Mg(NO_3)_2$ (0.5 g), NBu_4BF_4 (7.5 g) or tetrachloroplatinic(IV) acid (0.45 g), KCN (5.0 g), NBu_4BF_4 (3.5 g) in degassed acetonitrile (1 L each) were electrolyzed at direct current (20 nA) for 5 d. The cell was carefully rinsed twice with water and filled with a solution of NBu_4BF_4 (12.0 g) and $Mg(NO_3)_2$ (1.2 g) in degassed acetonitrile (1 L) for *I*(*V*) characteristic measurement.

Conclusion

Terminally aryl substituted long chain alkanethiols form highly ordered monolayers (SAMs) on gold surfaces. Mainly from RAIR-investigations and supported by molecular modeling it can be shown that the lateral SAM structure of the ω-phenoxy alkanethiols **2** on gold is perfectly ordered with optimal π-stacking of the aromatic rings and phenoxy-phenoxy distances in both dimensions which fit completely into the package of the alkyl chains and their placement on the gold surface. The strong π-interactions of the terminal aromatic rings do not only favor the perfect order of the SAMs but also "densify" their surface, markedly hindering the penetration of metals. Since phenoxy terminated SAMs were found to be perfect insulators, they can be applied for construction of stable and easy to handle ⟨metal-insulator-metal⟩ (MIM) junctions. The *I*(*V*) characteristics of ⟨gold-SAM-gold⟩ junctions have been measured depending on the chain length of compounds **2**. From the measured *I*(*V*) characteristics and simulation with theoretical tunneling models, a tunneling mechanism of the electrical conduction through thin organic layers is unequivocally confirmed experimentally.

The outstanding insulator properties of SAMs with terminal aryl substituents are not limited to gold as metal surface. Comparable results were obtained also with silicon surfaces by applying ω-phenoxy alkyl trichlorosilanes as SAM forming compounds.[16c,24] It was possible for example to prepare organic thin film transistors (TFTs) with the corresponding SAMs as gate dielectric and a high mobility organic semiconductor (pentacene).[25] These TFTs operate with supply voltages of less than 2 V, yet have gate currents that are lower than that of advanced silicon field-effect transistors with SiO_2 dielectrics.[25]

Supporting Information Available: Spectroscopic and analytical data. This material is available free of charge via the Internet at http://pubs.acs.org.

JA0548992

(24) (a) Schütz, M. Dissertation, Universität Stuttgart 2002. (b) Rittner, M. Dissertation, Universität Stuttgart 2002.
(25) Halik, M.; Klauk, H.; Zschieschang, U.; Schmid, G.; Dehm, Ch.; Schütz, M.; Maisch, S.; Effenberger, F.; Brunnbauer, M.; Stellacci, F. *Nature* **2004**, *431*, 963−966.